coatings

MDPI

Article

Improvement of Load Carrying Capacity of Concrete Pavement Slabs Using Macro Synthetic Fibers

Mohamed S. Eisa *, Mohamed E. Basiouny and Ahmed M. Youssef

Benha Faculty of Engineering, Benha University, Benha 13512, Egypt;
mohamed.bassyoni@bhit.bu.edu.eg (M.E.B.); ahmed.esmaiel18@beng.bu.edu.eg (A.M.Y.)
* Correspondence: mohamedeisa524@bhit.bu.edu.eg

Abstract: This study presents the results of an investigation of the effect of macro synthetic fibers (MSF) reinforcement on the load carrying capacity of concrete pavement slabs. Six concrete slabs having dimensions of 800 × 800 × 50 mm^3 were prepared and tested under static loads at three different positions: interior, edge and corner of the slab. Three of the slabs were Portland cement concrete (PCC) and prepared as references. The other three slabs were macro synthetic fiber reinforced concrete (MSFRC). Mechanical properties examined in this study included compressive strength, splitting tensile strength, flexural strength and modulus of elasticity and ductility of PCC and MSFRC. The findings showed that the addition of MSF to PCC improved the load carrying capacity of concrete pavement slabs. Test results obtained indicated that the ultimate load carrying capacity of MSFRC slabs was increased by 24%, 20%, and 23% for interior, edge and corner loading positions, respectively.

Keywords: macro synthetic fiber; concrete pavement; slabs; load carrying capacity

Citation: Eisa, M.S.; Basiouny, M.E.; Youssef, A.M. Improvement of Load Carrying Capacity of Concrete Pavement Slabs Using Macro Synthetic Fibers. *Coatings* **2021**, *11*, 833. https://doi.org/10.3390/coatings11070833

Academic Editor: Giuseppe Cantisani

Received: 9 June 2021
Accepted: 7 July 2021
Published: 10 July 2021

1. Introduction

Concrete pavement is subjected to repeated axle loads during its service life. Axle loads, which influence the rigid pavement, produce different stresses according to the different positions of the pavement [1]. The initiation of cracks may be caused due to the repeated application of axle loads along with the variation of temperature at the highly stressed positions. There are three critical positions: interior, edge and corner, which influence the structural performance of pavement [2–6]. The propagation of cracks through the concrete pavement—especially for these positions—causes fracture and failure, which can lead to loss of serviceability and unsafe driving conditions [6,7]. This occurrence is mainly because of the brittleness of concrete together with its small toughness and its low resistance to fatigue [7]. Therefore, researchers started to modify the concrete permanently, to enhance its comprehensive performance. They have found an effective and economic way of enhancement. By mixing of concrete and different types of fibers, a new type of building material with brilliant comprehensive performance is produced, namely fiber reinforced concrete (FRC) [8].

Many studies have been conducted in the last decades concerning the mechanical performance of FRC. It appears that the incorporation of fibers in the concrete mixture could considerably enhance the mechanical properties of concrete [9–12]. Furthermore, fibers have been used to enhance the cracking performance of concrete pavements, provide additional structural capacity and decrease the required slab thickness [13].

There are mainly four types of fibers that can be used to reinforce concrete: steel fiber, glass fiber, natural fiber and synthetic fiber [14]. Recently, synthetic fiber has been more famous due to its excellent comprehensive characteristics. Compared to other fibers, synthetic fiber has been widely used in engineering practice, with the properties of small density, appropriate price and easy dispersion in concrete [15]. Synthetic fiber can be made of polyolefin, aramid, acrylic and carbon [16].

Synthetic fiber is classified into two categories according to its diameter, i.e., the fiber with a diameter less than and that with a diameter more than 0.3 mm, referred to as micro synthetic and macro synthetic fiber, respectively [17]. Based on this classification, synthetic fiber provides two levels of performance in the process of cracking. At the level of material, the ductility and strength of the concrete can be improved by using microfiber. At the structural level, the ductility and load carrying capacity of the structure can be enhanced by the incorporation of macro fiber [18].

Macro synthetic fiber has considerably enhanced in the past decade, and can now be used in structural applications [19]. Due to their crimped shape as well as their low modulus of elasticity, macro synthetic fibers exhibit higher deformation at failure load, post-cracking load carrying capacity, toughness, and decreased width of cracks [20]. Multiple laboratory-scale slab tests with macro synthetic fiber reinforcement have presented that the ultimate load carrying capacity of FRC slabs considerably increased relative to plain concrete slabs [21,22].

Among different types of synthetic fiber, polymer fiber is more popular than the other. This polymeric fiber can provide long-term durability in aggressive conditions, due to its hydrophobicity and excellent chemical stability. Polypropylene (PP) fiber is the main member of the polymer-based fiber used in concrete [23,24]. PP fiber is family in the subcategory of polyolefin [25]. PP fiber has been attracting the attention of researchers because of its lower weight and cost, excellent toughness, resistance to corrosion and acids, and improved resistance to shrinkage cracking [26,27].

Many researchers have investigated the properties of concrete incorporating PP fiber. PP fiber reinforced concrete (PPFRC) showed no considerable enhancement in compressive strength, but considerable enhancement in tensile and flexural strengths and modulus of elasticity [28,29]. The incorporation of PP fiber in the concrete mixture could considerably enhance the energy absorption, durability, toughness and ductility of concrete, and enhance its resistance to shock, abrasion and fatigue [30,31]. Furthermore, crack width in concrete pavement and slabs on grade could be restricted by using PP fiber in concrete [32]. As a result, PPFRC appears to be a very attractive concrete pavement matrix, with special regard to high performance and safety [7]. There are many types of PP fiber which are manufactured with different length, diameter and physical properties [33]. A new type of MSF i.e., structural macro synthetic polypropylene fiber is manufactured by different manufacturers, and it is gaining popularity to enhance the mechanical properties of concrete.

The structural macro synthetic polypropylene fibers are produced with specific improvements to surface in the form of indentations and textured finishes, to optimize the bond with concrete. Embossed structural macro synthetic polypropylene fibers provide substantial post-peak load carrying capacity and continued resistance with increasing crack separation [34]. Another significant benefit is the post-cracking performance provided by the structural macro synthetic polypropylene fibers. Brittle plain concrete has no effective post-cracking ductility, but the structural macro synthetic polypropylene fibers can significantly improve the post-cracking response of concrete, because the structural macro synthetic polypropylene fibers act as a crack arrester, and alter the intrinsically brittle concrete matrix into a tough material with better crack resistance and ductility. Therefore, when concrete breaks, the common large single cracks can be substituted with dense micro-cracks due to the existence of structural macro synthetic polypropylene fiber reinforcement [16]. Furthermore, adding structural macro synthetic polypropylene fibers to concrete mixes led to ductile failure of concrete specimens. This is because fibers bridge at cracked sections and prevent sudden failure. At the cracked section, fibers handle the load and restore the load into the concrete section. The bridging mechanism of structural macro synthetic polypropylene fibers is better due to their length [35].

To the author's best knowledge, no study has been conducted on the use of structural macro synthetic polypropylene fiber reinforced concrete (MSFRC) for the application of concrete pavements. The mechanical properties of MSFRC were investigated in this study and compared with that of the conventional mix. The mechanical properties of concrete

were investigated by measuring compressive, splitting tensile and flexural strengths and modulus of elasticity and ductility. Furthermore, to evaluate the performance of using MSFRC in concrete pavement slabs, the ultimate load carrying capacities and vertical deflections were calculated at the interior, edge and corner positions on the concrete slab.

2. Experimental Program

2.1. Materials

2.1.1. Cement

The cement used in this study was ordinary Portland cement type I (CEM-I 42.5 N) according to the EN 197-1 standard [36]. Table 1 shows the physical and mechanical properties of cement and the Egyptian standard specifications [37].

Table 1. The physical and mechanical properties of cement.

Property	Value	Specifications [37]
Soundness	1.0	≤10
Initial setting time (min)	150	≥60
Final setting time (min)	195	-
Specific surface area (m^2/kg)	385	-
Flexural strength @ 2 days (MPa)	4.8	-
Flexural strength @ 28 days (MPa)	7.6	-
Compressive strength @ 2 days (MPa)	19.5	≥10
Compressive strength @ 28 days (MPa)	48.3	42.5 ≤ X ≤ 62.5

2.1.2. Aggregate

Locally available crushed stone from the Suez Attaka quarry of sizes 20 mm and 10 mm in 50:50 proportion was used as coarse aggregate, and natural sand was used as fine aggregate. Table 2 shows the physical properties of coarse, fine aggregates and the Egyptian standard specifications [38].

Table 2. Properties of aggregate.

Property	Crushed Stone Aggregate	Fine Aggregate	Specifications [38]
Bulk density (g/cm^3)	1.65	1.56	-
Fine particles percent (%)	1.2	1.1	≤2.5%
Water absorption (%)	1.6	1.39	≤2.5%
LA abrasion (%)	23.7	-	≤30% (for crushed stone)
Shape index (%)	8.4	-	≤25%
Flakiness index (%)	12.4	-	≤25%

2.1.3. Water and Superplasticizer (SP)

For casting and curing purposes, potable water was used in PCC and MSFRC mixtures. The superplasticizer used in this study was polycarboxylic ether (PCE), provided by BASF, and complied with the ASTM C494 standard [39]. The superplasticizer was used to facilitate the dispersion of MSF in the concrete mixture, and to attain the desired workability for concrete [40].

2.1.4. Fibers

The synthetic fibers were chosen based on the present market trend and the findings of a literature review. The structural macro synthetic polypropylene fibers were found to be the most desirable and sustainable. The fibers were extruded from a natural PP homopolymer according to the ASTM C1116 [41] and EN 14889-2 [42] standards. The MSF used in this study were manufactured by BASF Construction Chemicals, Dubai, with a trade name Master fiber 249. The fiber manufacturer provided the material properties and

dosage of the MSF, which can be found in the datasheet published on the BASF website [43]. These PP fibers were straight strips with a continuously embossed surface texture and were highly resistant to chemicals and alkali. Further details about the properties of MSF, as provided by the manufacturer [43], are reported in Table 3. Figure 1 shows the shape of the MSF used in this study.

Table 3. Properties of structural macro synthetic polypropylene fibers.

Properties	Value
Material	Polyolefin 100%
Design	Monofilament
Specific gravity	0.91
Equivalent diameter	0.85 mm
Length	48 mm
Aspect ratio	56.6
Tensile strength	400 MPa
Modulus of elasticity	4.7 GPa
Water absorption	Nil
Shape	Elliptical
Melting point	160 °C
Ignition point	350 °C

Figure 1. Structural macro synthetic polypropylene fibers.

2.2. Mixing, Casting and Curing Procedure

A pan mixer (MATEST manufacturer, Treviolo, Italy) with a capacity of 0.1 m^3 was used for mixing. To cast all the specimens, two batches were prepared with the same mix proportions. The first batch was used to cast all PCC specimens, while the second batch was used to cast all MSFRC specimens. The ratio of water to cement (w/c) used in PCC and MSFRC mixtures was 0.45. A mixture without any MSF was prepared as a control. To produce PCC, the process of mixing began with the dry mixing for 30 s of the coarse and fine aggregates. Then, the cement was added to the mixture and blended for 1 min. Subsequently, for 30 s, a liquid mixture of water and SP was poured into the mixture. To attain the desired workability for concrete, the obtained mixture was then stirred for 2 min.

In the other mixture, MSF were added to the PCC at a constant dosage of 6 kg/m^3 corresponding to a volume fraction (V_f) of 0.66%. This dosage was selected, as (a) the dosage suggested by the manufacturer to attain appropriate performance [43], and (b) based on previous studies [44–48]. Table 4 shows the proportions of the concrete mixture. In the MSFRC mixture realized as part of this study, the same proportions were retained for the concrete matrix. The amount of SP was remained the same for PCC and MSFRC mixtures at 1.0% of the cement weight to assess the influence of MSF on the concrete

mixture workability. MSF were typically added to the ready-mix concrete in the batch plant, and the produced concrete was easy to pump and implement [49]. In this study, MSF were added after mixing aggregates, cement, and water. Then, for 2 min, the mixture was thoroughly mixed to ensure uniform distribution. Two minutes of additional mixing was sufficient for the appropriate dispersion of MSF in the mixture without leading to a "balling" influence [50].

Table 4. Proportions of concrete mix (Unit: kg/m^3).

Type of Mixture	Cement	Sand	Agg. #10	Agg. #20	Water	SP	Fiber
PCC	400	740	530	530	175	5.7	-
MSFRC	400	740	530	530	175	5.7	6

For each mixture, the fresh properties of concrete were measured after the mixing procedure. Six timber formworks were prepared for molding of concrete slabs. Figure 2 shows the concrete slabs prepared for this study. All slabs were cast on the same day and were compacted using mechanical vibrators (MATEST manufacturer, Treviolo, Italy). The slabs were cured for 28 days after 24 $\pm$ 2 h from the casting. To prevent losing moisture from the concrete, the slabs were covered with hessian blankets during the curing process. Additionally, to minimize the effects of ambient air, the slabs were covered with two layers of plastic sheets.

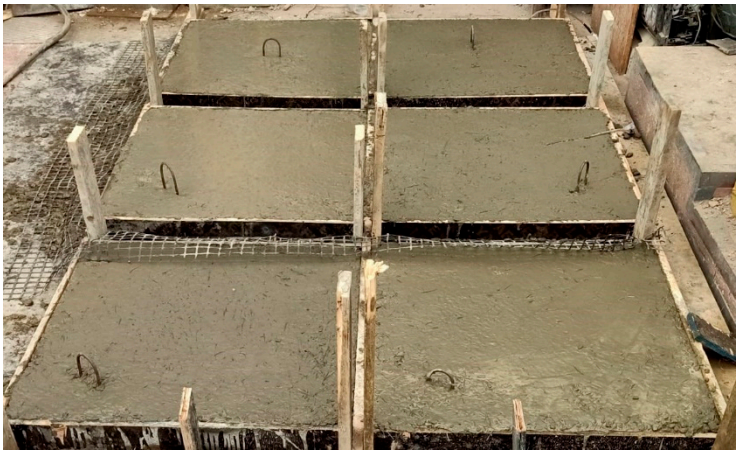

Figure 2. Concrete slabs.

In addition to the slabs, PCC and MSFRC specimens were also cast for the companion mechanical tests. For each mixture, the fresh concrete was cast into cubic molds of size 100 mm, cylindrical molds with the dimensions of 150 mm diameter by 300 mm height, and prismatic molds having a size of 100 $\times$ 100 $\times$ 500 mm^3, as shown in Figure 3. The specimens were cast in two layers and vibrated on a vibrating table for 25 s per layer. To avoid moisture loss, the specimens were covered with plastic sheets after casting. Then, the specimens were kept under standard laboratory conditions for 24 $\pm$ 2 h until demolding. Subsequently, the specimens were placed in a curing tank (23 $\pm$ 2 °C and 95% $\pm$ 5% relative humidity (RH)) until testing. All tests were performed at 28 days.

Figure 3. Concrete specimens.

3. Test Procedures

3.1. Fresh Properties

The slump, air content and fresh density were calculated immediately after the mixing process according to the ASTM C143 [51], ASTM C231 [52], and ASTM C138 [53] standards, respectively.

3.2. Compressive Strength Test

The compressive strength tests were conducted on three 100 × 100 × 100 mm^3 cubic specimens for each mixture at 28 days according to the EN 12390-3 standard [54]. The compression testing machine used was an ELE (Engineering Laboratory Equipment) of capacity 2000 kN. For each mixture, the average of three compressive strength values was reported.

3.3. Splitting Tensile Strength Test

The splitting tensile test is well known as one of the simplest and most dependable tests for the indirect evaluation of concrete tensile strength [55]. The splitting tensile strength tests were conducted on cylindrical concrete specimens of 150 mm diameter and 300 mm height at 28 days according to the ASTM C496 standard [56]. The load was applied continuously at a constant rate up to failure using a universal testing Schmadzu-machine of capacity 500 kN. The failure load was reported to calculate the splitting tensile strength by following Equation (1), and three specimens were used to calculate the average strength.

$$F_{sp} = \frac{2P}{\pi dl} \quad (1)$$

where, F_{sp} = splitting tensile strength (MPa), P = failure load (N), d = cylinder diameter (mm), and l = cylinder height (mm).

3.4. Flexural Strength Test

Flexural strength, sometimes also known as modulus of rupture (MOR), is like an evaluation of tensile strength in bending. The flexural strength tests were conducted on 100 × 100 × 500 mm^3 prism test specimens at 28 days, according to the ASTM C293 standard [57]. For each mixture, three specimens were prepared, and the average values were recorded. The set-up consists of two supporting rollers, spaced by 400 mm, and one loading roller placed in the middle. The flexural test was conducted using a universal testing Schmadzu-machine of capacity 500 kN. Equation (2) was used to calculate the flexural strength of the concrete specimens.

$$F_b = \frac{3Pl}{2bh^2} \quad (2)$$

where F_b = flexural strength (MPa), P = failure load (N), l = specimen span (mm), b = specimen width (mm) and h = specimen height (mm).

3.5. Modulus of Elasticity Test

Modulus of elasticity is an important mechanical property used to evaluate the behavior of concrete [58]. Modulus of Elasticity was calculated by averaging the test results of three 150 × 300 mm^2 cylindrical specimens for each mixture at 28 days according to the ASTM C469 standard [59]. In this test, the cylindrical specimens were subjected to compressive loading in the longitudinal direction. The axial stress of the specimens during the compression test was determined as the ratio of the applied compressive force to the specimens' cross section, and their axial strain was also calculated through measurement of the axial deformation at the mid-height.

3.6. Slabs Loading Test

Table 5 presents the details of PCC and MSFRC slabs. Six concrete slabs, having dimensions of 800 × 800 × 50 mm^3, were prepared and tested under a static load. Three of the slabs were PCC slabs and taken as references. The other three slabs were MSFRC slabs. The slabs were divided into three groups according to the position of the applied load. Each group consisted of two slabs (PCC and MSFRC slabs). The load was applied at the interior of the slabs for the first group. The load was applied at the edge of the slabs for the second group. For the third group, the slabs were tested by applying the load at the corner of the slab.

Table 5. Details of slabs.

Slab Type	Loading Position	Slab Label	Dimensions (mm)	Restraints
PCC	Interior Edge Corner	PI PE PC	800 × 800 × 50	Springs with k = 37 MPa/m
MSFRC	Interior Edge Corner	FI FE FC	800 × 800 × 50	Springs with k = 37 MPa/m

The number of six concrete slabs chosen in this study was to test one slab for one position for PCC and MSFRC slabs as simulated in a study performed in 1998 [60], and another one in 2018 [61]. They studied the behavior of concrete pavement slabs with one slab for each case of the loading position with consideration the ratio of side dimension to thickness, more than 15 times that complied with concrete pavement design assumptions reported by the Portland cement association (PCA) [62].

The labelling of PCC and MSFRC slabs is summarized in Table 5. The first letter in the table is PCC slabs (P) (reference) and fiber reinforced concrete slabs (F). The second letter on the label refers to the position of the applied load, which are interior, edge and corner labelled as (I), (E) and (C), respectively. For example, the MSRFC slab which was loaded at the edge of the slab is labelled as (FE).

To simulate a subgrade soil with a specific modulus of subgrade reaction, steel springs were used under a layer of recycled rubber with a 20 mm thickness that was used to ensure the uniform distribution of stress overall springs. A displacement control testing machine was used to calculate the springs' modulus of reaction or spring constant in compression by recording the applied loads with the regarding displacements. The average modulus of subgrade reaction of the springs was 37 MPa/m.

Figure 4 shows the concrete slab loading frame. The load was monotonically applied by a hydraulic jack of capacity 1000 kN. A circular steel disk with a 100 mm diameter was placed between the hydraulic jack and the slab. The load was applied until the collapse load of the slab was reached. A steel frame was used to fix the concrete slabs with spring support while applying the load. The steel frame contained three steel angles with dimensions of

$50 \times 50 \times 5$ mm^3 and one steel strip to fix the fourth side of the slab. Figure 5 shows the test set-up for the three load cases.

Figure 4. Concrete slab loading frame.

(**a**) (**b**) (**c**)

Figure 5. Test set-up for the three load cases: (**a**) Interior; (**b**) Edge; (**c**) Corner.

The parameters measured during the monotonic testing were the slab vertical deflection and the applied load. The deflection that occurred at the loaded area was measured by linear variable displacement transducers (LVDTs). The maximum applied load which caused the collapse of the slab was defined as the ultimate load carrying capacity. The load versus deflection curves were plotted for different loading positions for each slab.

4. Test Results and Discussion

4.1. Fresh Concrete Properties

The fresh properties of PCC and MSFRC mixtures were measured, and the results are reported in Table 6. The addition of fibers is well known to have a major effect on PCC workability [63]. In this study, the amount of water and SP remained the same for PCC and MSFRC mixtures to assess the effect of MSF on MSFRC workability. From Table 6, it can be noted that the slump of 112 mm was obtained for the PCC, and once the MSF were added, the slump reduced by 27.6% compared with that of PCC. This reduction in slump can be because of the use of fibers that can create a network structure in the concrete mixture, consequently preventing the mixture from segregation and flow [63]. Furthermore, because of the large surface area of fibers, fibers can absorb cement paste to wrap around, consequently increasing the viscosity of the concrete mixture and reducing its workability [64].

Table 6. Fresh concrete properties.

Mixture ID	Slump (mm)	Air Content (%)	Density (kg/m^3)
PCC	112	1.7	2389
MSFRC	81	1.9	2332

In the case of air content, as reported in Table 6, the added MSF participated in the increase of air content. PCC showed air content of 1.7%, and MSFRC showed higher air content of 1.9%. During the mixing process, fibers can entrap more air [65]. The large specific surface area of the fibers and their trend to sometimes conglomerate can also participate in the increase of air entrapment [66].

The densities of PCC and MSFRC were 2389 and 2332 kg/m^3, respectively, as reported in Table 6. The density of MSFRC was reduced by 58 kg/m^3 than that of PCC. Consequently, the density of MSFRC was reduced by 2.4% as compared to that of PCC. The less density of MSFRC than that of PC is due to the existence of less density of MSF [37]. Moreover, the above-mentioned increase in air content may have a slight impact on the density [65].

4.2. Compressive Strength

Figure 6 presents the results of compressive strength of PCC and MSFRC specimens at 28 days. Each mixture achieved the target compressive strength of 30 MPa. The 28-day compressive strength of PCC was 34.6 MPa. With the incorporation of MSF, the compressive strength was not significantly influenced, which was minor reduced by about 4% compared with that of PCC specimens. In previous studies [24,67], researchers reported a 6%–13% decrease in compressive strength of concrete due to the addition of other types of MSF. This decrease could be because of the existence of voids due to the incorporation of MSF and the presence of weak interfacial bonds between MSF and cement particles [68]. Moreover, this reduction may be due to the influence of MSF on decreasing the mixture density [51].

There was a change in the failure mode of the specimens when MSF were added. The failure mode significantly changed from brittle to ductile. The cubic specimens did not crush but held their integrity up to the end of the test due to the bridging effect of fibers [49,69].

4.3. Splitting Tensile Strength

The results of the splitting tensile strength at 28 days are presented in Figure 7. As can be noted from the results, the splitting tensile strength of MSFRC specimens was increased when compared with that of PCC specimens. The results clarified that the incorporation of MSF enhanced the splitting tensile strength of MSFRC specimens by about 20.5%, in comparison with that of PCC specimens. In previous studies [70,71], researchers reported a 12%–16% increase in splitting tensile strength of concrete with the addition of other types of MSF.

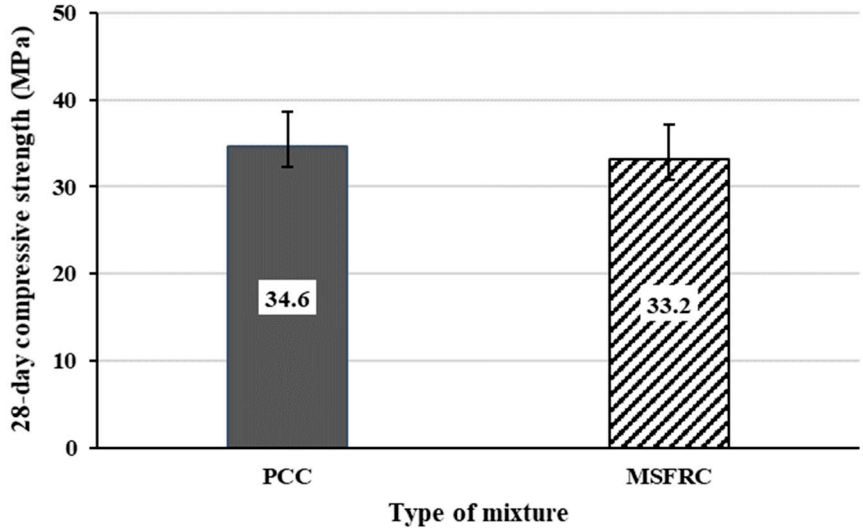

Figure 6. Compressive strength test results.

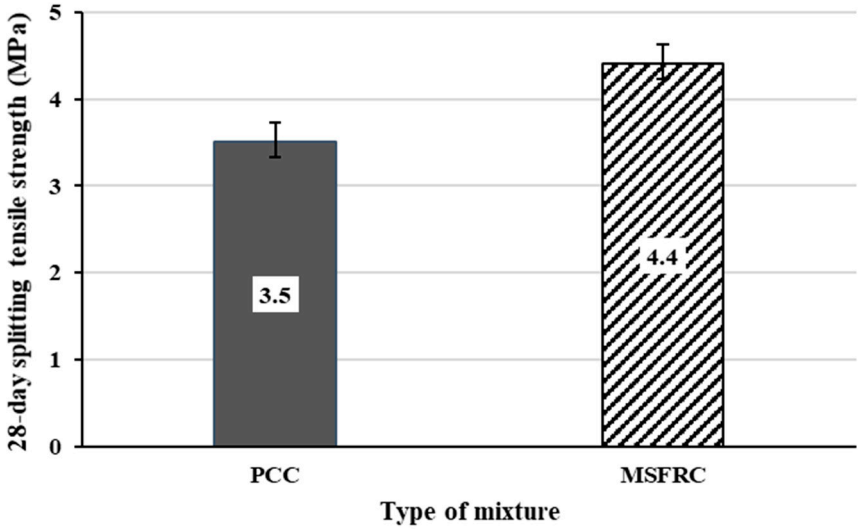

Figure 7. Splitting tensile strength test results.

Even if the MSF have significant tensile strength, the brittle concrete is not designed to withstand the tensile force, and therein crack initiation is still restricted by the quality of the cement matrix, the peak load usually occurred when the main crack happened in the concrete. However, after the crack occurred, the effect of fiber bridging could provide an important role in restricting the fast growth of the crack. Consequently, MSF did not clearly enhance the PC splitting tensile strength, but it significantly participated in the crack restricting [65].

Behaviors of distinct failure of concrete specimens were noticed after the test of splitting tensile. The PCC specimen displayed the obvious brittle failure as shown in Figure 8. However, after the addition of MSF, the failure behavior of the MSFRC specimen was varied; the failure was gradual, and the two parts were not fully separated. The morphology of the fracture confirmed that the MSF can bridge the crack and keep the concrete specimen to carry significant load after the occurrence of the first crack.

(**a**) (**b**)

Figure 8. The fracture sample morphology: (**a**) failed PCC specimen; (**b**) failed MSFRC specimen.

4.4. Flexural Strength

Figure 9 presents the results of the 28-day flexural strength test of PCC and MSFRC specimens. The results reported that adding MSF increased the flexural strength of PCC. The flexural strength of PCC was 8.3 MPa and the addition of MSF increased it by about 33%. In previous studies [72,73], researchers reported a 13%–17% increase in flexural strength of concrete with the addition of other types of MSF. It may be due to the bridging mechanism of MSF which restrained cracks growth and decreased crack width.

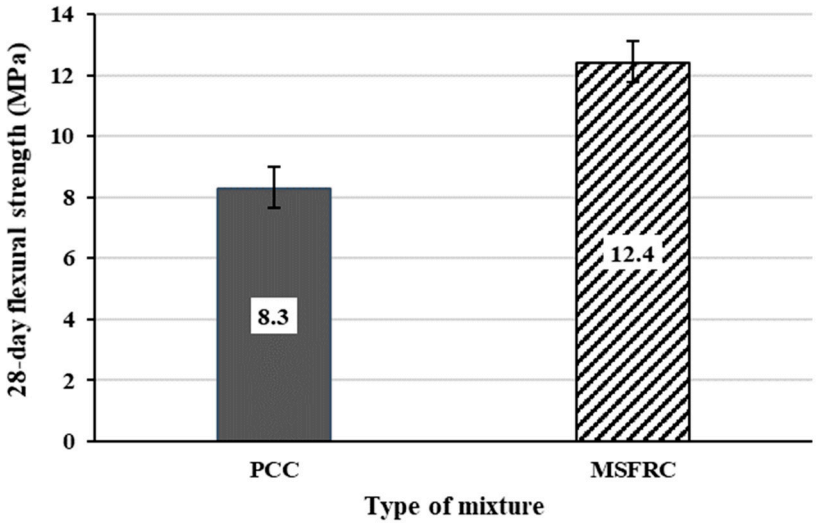

Figure 9. Flexural strength test results.

Figure 10 displays the cracking mechanism of concrete specimens under the flexural test. It was observed that the PC specimen broke at the maximum load into two parts, displaying brittle behavior. Brittle behavior is permanently related to PCC [74]. The specimen cracked and collapsed almost suddenly when the first crack occurred, with very little deformation and no preceding warning. On the other hand, in the MSFRC specimen, the failure progressed with bending, but without any sudden collapse as observed in the PCC specimen. The load was transferred to the MSF when the concrete failed. The MSF restrained the growth of cracks and consequently delayed the failure [75].

(**a**) (**b**)

Figure 10. Cracking mechanism of concrete specimens under flexural strength test: (**a**) PCC (**b**) MSFRC.

4.5. Modulus of Elasticity

Figure 11 presents the results obtained for the modulus of elasticity of PCC and MSFRC specimens. According to Figure 11, an increase in the 28-day modulus of elasticity was observed by 6% for MSFRC specimens as compared to PCC specimens. In a previous study [42], researchers observed a 3% increase in the modulus of elasticity of concrete reinforced with another type of MSF. By adding MSF, because of their embossed surface, a strong coherence was developed in the concrete specimen, which in turn improved the modulus of elasticity of the MSFRC with respect to the PCC [42]. Furthermore, MSF arrested the original shrinkage cracks in the concrete and hence reduced the strain induced under compression loading, and then enhanced the modulus of elasticity of MSFRC [76,77].

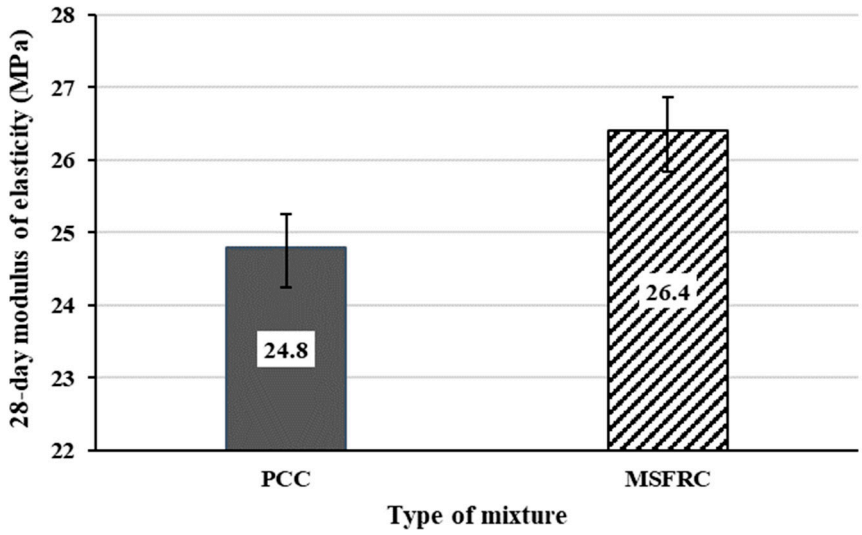

Figure 11. Modulus of elasticity test results.

The performance properties of plain concrete pavement were obtained for different values of elastic modulus of concrete ranging from 24 to 35 GPa [78]. Concrete with a higher elastic modulus behaved in a better way to deal with the loading stresses as compared with concrete with lower elastic modulus [78]. Therefore, the improvement in elastic modulus can be beneficial in concrete pavement design. It can be beneficial to increase the ultimate load capacity of PCC slabs, if the same thickness of PCC slabs will be used with reinforcement of MSF for the same service life [79].

4.6. Slabs Loading

Table 7 shows the test results of PCC and MSFRC slabs. The maximum applied load of PCC slabs ($P_{ref.}$) and MSFRC P_{FRC} are reported in this table. Also, Table 7 shows the deflections of PCC slabs ($\Delta_{ref.}$ and MSFRC slabs (Δ_{FRC} that occurred at the loaded area. The expression of $[\{(P_{FRC}/P_{ref.}) - 1\} \times 100]$ was used to calculate the increase of load carrying capacity of the MSFRC slabs compared to the PCC slabs, as reported in Table 7. The ductility of the tested concrete slabs is one of the investigated parameters in this study. It is defined as the ability of the specimen to resist the applied load from the start of loading until the failure occurred. It was determined by calculating the area under the applied load versus the deflection curve (Figures 12–14), as listed in Table 7.

Table 7. Experimental results for tested slabs.

Slab Label	$P_{ref.}$ (kN)	P_{FRC} (kN)	$\Delta_{ref.}$ (mm)	Δ_{FRC} (mm)	$\{(P_{FRC}/P_{ref.}) - 1\} \times 100$ (%)	Ductility (%)
PI	735	-	13.1	-	-	-
PE	587	-	25.5	-	-	-
PC	668	-	29.2	-	-	-
FI	-	971	-	16.7	24	43
FE	-	732	-	27.6	20	26
FC	-	868	-	31.3	23	33

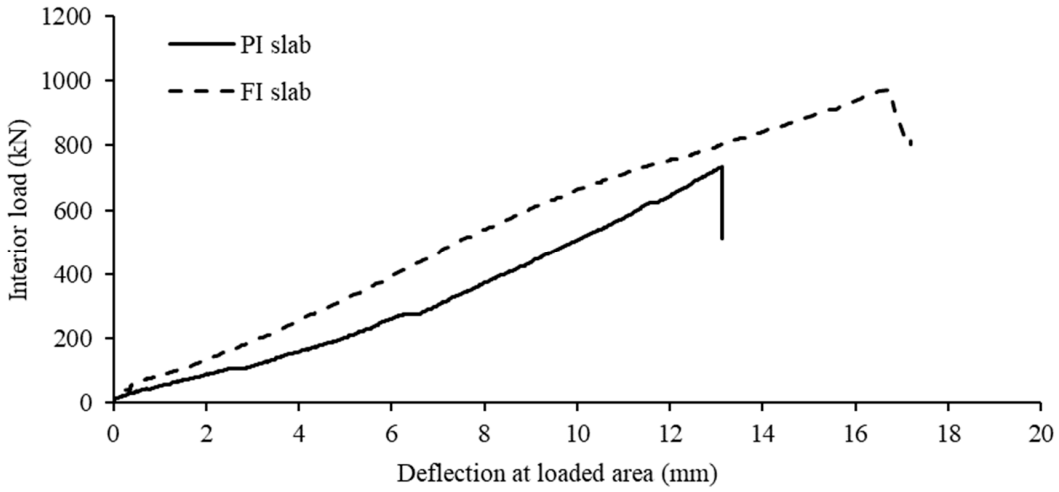

Figure 12. Interior load versus deflection at the loaded area of PCC and MSFRC slabs.

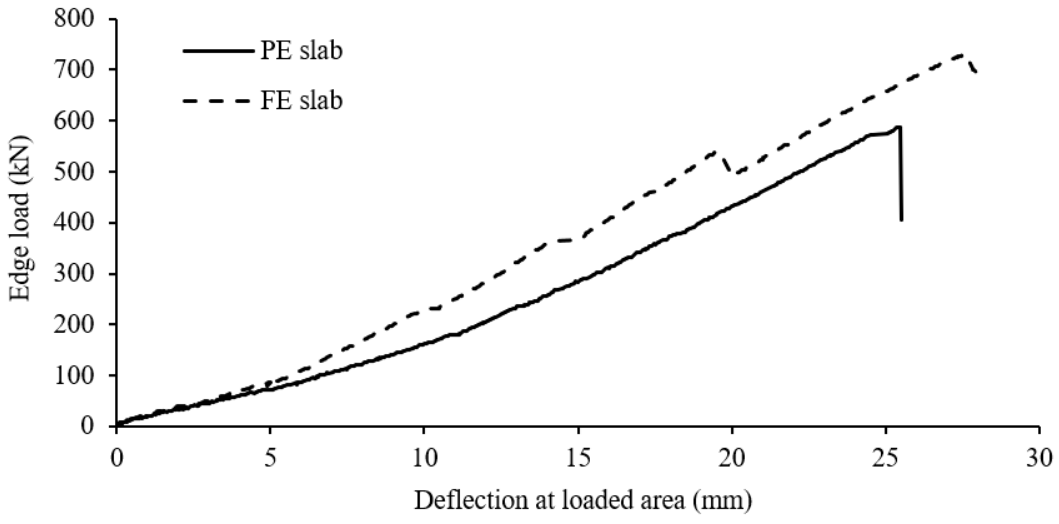

Figure 13. Edge load versus deflection at the loaded area of PCC and MSFRC slabs.

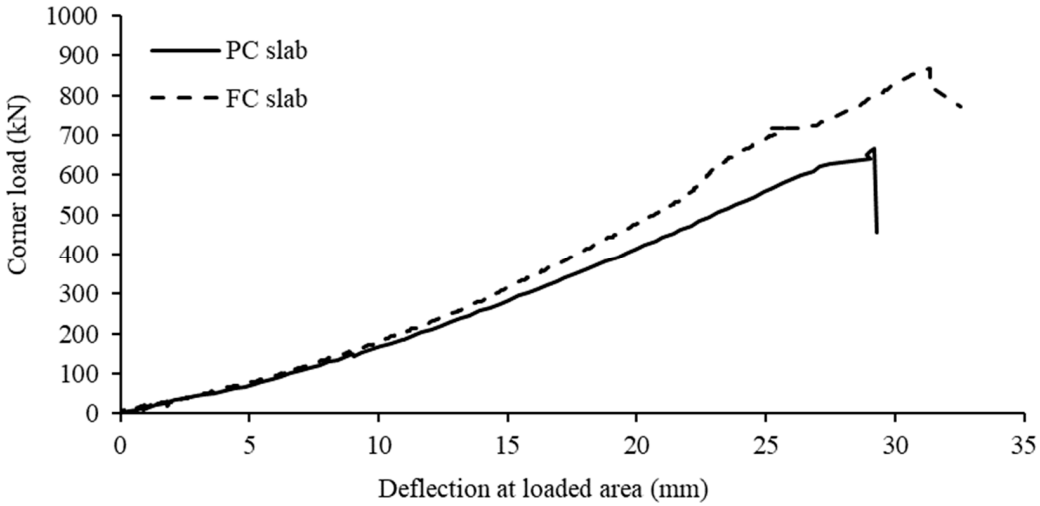

Figure 14. Corner load versus deflection at the loaded area of PCC and MSFRC slabs.

The interior applied load versus deflection curves of PCC and MSFRC slabs, which were tested by applying a load at the interior of the slabs, labelled as slabs PI and FI, respectively, are shown in Figure 12. During the application of load, the ultimate applied load of slab PI was 735 kN. Meanwhile for slab FI, the ultimate load was 971 kN. This achieved an increase in the load carrying capacity of slab FI by about 24% more than slab PI. In addition, this achieved an increase in the ductility of slab FI by about 43% more than slab PI. The recorded deflection that occurred for slab PI was 13.1 mm. Meanwhile for slab FI, the maximum deflection was 16.7 mm.

For PCC and MSFRC slabs, which were tested by applying a load at the edge of the slab, named as slabs PE and FE, respectively, Figure 13 presents the edge applied load versus deflection curves that occurred at the loaded area. The ultimate applied load was 587 kN for slab PE. For slab FE, the ultimate load was 732 kN. This increase attained improvement in the load carrying capacity of slab FE by about 20% more than slab PE. In addition, this increase attained improvement in the ductility of slab FE by about 26% more than slab PE. The deflection of slabs PE and FE was 25.5 and 27.6 mm, respectively.

Figure 14 shows the curves of corner applied load versus deflection that occurred at the loaded area for PCC and MSFRC slabs, which were tested by applying a load at the corner of the slabs, named as slabs PC and FC, respectively. The ultimate applied load was 668 kN for slab PC. For slab FC, the ultimate applied load was 868 kN. This achieved an increase in the load carrying capacity of slab FC by about 23% more than slab PC. In addition, this achieved an increase in the ductility of slab FC by about 33% more than slab PC. The maximum deflection was 29.2 mm for slab PC and 31.3 mm for slab FC.

The essential mechanism allowing for an increased collapsed load for MSFRC slabs was associated with the ability of fibers to engage a large proportion of the concrete slab in carrying and distributing load even after the occurrence of cracking [21].

5. Conclusions

Based on the results of this study, the following conclusions can be drawn:

1. Adding MSF to the concrete mixture led to reduced workability of the fresh concrete.
2. It was observed that concrete density was not mainly affected by the addition of MSF.
3. The addition of MSF caused a slight increase in air content as compared to the PCC.
4. The addition of MSF did not have a considerable effect on compressive strength, as by adding MSF to the concrete mix, a 4% decrease in compressive strength was observed.
5. The splitting tensile strength, flexural strength and elastic modulus of MSFRC at 28 days were increased by 20.5%, 33% and 6%, respectively, compared with that of PPC.

6. The load carrying capacity of the PCC slab was improved considerably by the addition of MSF.
7. The load carrying capacity of the MSFRC slab was higher than the PCC slab by about 24% for interior loading, 20% for edge loading and 23% for corner loading.
8. The ductility of the MSFRC slab was higher than the PCC slab by about 43% for interior loading, 26% for edge loading and 33% for corner loading.
9. In general, the results obtained and the observations made in this study proposed that concrete incorporating MSF could be used with satisfactory mechanical properties to increase the load carrying capacity and ductility of rigid pavement slabs.

Author Contributions: Conceptualization, M.S.E.; Methodology, A.M.Y.; Writing—review & editing, M.E.B. All authors have read and agreed to the published version of the manuscript.

Funding: This research received no external funding.

Institutional Review Board Statement: Not applicable.

Informed Consent Statement: Not applicable.

Data Availability Statement: All data presented in this study are available within this article.

Acknowledgments: The authors are thankful to the teamwork of the General Authority for Roads, Bridges and Land Transport—GARBLT, Egypt.

Conflicts of Interest: The authors declare no conflict of interest.

References

1. Tunç, A. *Yol Malzemeleri ve Uygulamaları*; Atlas Yayınevi: Istanbul, Turkey, 2001.
2. Kim, Y.K.; Lee, S.W. Performance evaluation of bonded concrete overlay. *Constr. Build. Mater.* **2013**, *49*, 464–470. [CrossRef]
3. Lee, Y.-H. Corner stress analysis of jointed concrete pavements. *Transp. Res. Rec. J. Transp. Res. Board* **1996**, *1525*, 44–56. [CrossRef]
4. Lee, Y.H.; Yen, S.T.; Lee, C.T.; Bair, J.H.; Lee, Y.M. Development of new stress analysis and thickness design procedures for jointed concrete pavements. In Proceedings of the 6th International Conference of Concrete Pavements, Purdue University, West Lafayette, IN, USA, 18–21 November 1997.
5. Setyawan, A.; Zoorob, S.; Hasan, K. Investigating and comparing traffic induced and restrained temperature stresses in a conventional rigid pavement and semi-rigid layers. *Procedia Eng.* **2013**, *54*, 875–884. [CrossRef]
6. Tang, T.; Zollinger, D.G.; Senadheera, S. Analysis of concave curling in concrete slabs. *J. Transp. Eng.* **1993**, *119*, 618–633. [CrossRef]
7. Nobili, A.; Lanzoni, L.; Tarantino, A.M. Experimental investigation and monitoring of a polypropylene-based fiber reinforced concrete road pavement. *Constr. Build. Mater.* **2013**, *47*, 888–895. [CrossRef]
8. Chen, Y.; Cen, G.; Cui, Y. Comparative study on the effect of synthetic fiber on the preparation and durability of airport pavement concrete. *Constr. Build. Mater.* **2018**, *184*, 34–44. [CrossRef]
9. Mohammadi, Y.; Singh, S.P.; Kaushik, K.S. Properties of steel fibrous concrete containing mixed fibres in fresh and hardened state. *Constr. Build. Mater.* **2008**, *22*, 956–965. [CrossRef]
10. Yazıcı, Ş.; İnan, G.; Tabak, V. Effect of aspect ratio and volume fraction of steel fiber on the mechanical properties of SFRC. *Constr. Build. Mater.* **2007**, *21*, 1250–1253. [CrossRef]
11. Thomas, J.; Ramaswamy, A. Mechanical properties of steel fiber-reinforced concrete. *J. Mater. Civ. Eng.* **2007**, *19*, 385–392. [CrossRef]
12. Afroughsabet, V.; Biolzi, L.; Ozbakkaloglu, T. High-performance fiber-reinforced concrete: A review. *J. Mater. Sci.* **2016**, *51*, 6517–6551. [CrossRef]
13. Altoubat, S.A.; Roesler, J.R.; Lange, D.A.; Rieder, K.A. Simplified method for concrete pavement design with discrete structural fibers. *Constr. Build. Mater.* **2008**, *22*, 384–393. [CrossRef]
14. Daniel, J.I.; Gopalaratnam, V.S.; Galinat, M.A. *State-of-the-Art Report on Fiber Reinforced Concrete*; ACI Committee 544, Report 544, 1R-96; American Concrete Institute: Detroit, MI, USA, 2002.
15. Zheng, Z.; Feldman, D. Synthetic fibre-reinforced concrete. *Prog. Polym. Sci.* **1995**, *20*, 185–210. [CrossRef]
16. Yin, S.; Tuladhar, R.; Shi, F.; Combe, M.; Collister, T.; Sivakugan, N. Use of macro plastic fibres in concrete: A review. *Constr. Build. Mater.* **2015**, *93*, 180–188. [CrossRef]
17. American Concrete Institute (ACI). *Guide for Specifying, Proportioning, and Production of Fiber-Reinforced Concrete*; ACI 544.3R-08; ACI: Farmington Hills, MI, USA, 2008.
18. Rossi, P. High performance multimodal fiber reinforced cement composites (HPMFRCC): The LCPC experience. *Mater. J.* **1997**, *6*, 478–783.
19. Navas, F.O.; Navarro-Gregori, J.; Herdocia, G.L.; Serna, P.; Cuenca, E. An experimental study on the shear behaviour of reinforced concrete beams with macro-synthetic fibres. *Constr. Build. Mater.* **2018**, *169*, 888–899. [CrossRef]

20. Yang, J.-M.; Min, K.-H.; Shin, H.; Yoon, Y.-S. Effect of steel and synthetic fibers on flexural behavior of high-strength concrete beams reinforced with FRP bars. *Compos. Part B Eng.* **2012**, *43*, 1077–1086. [CrossRef]
21. Roesler, J.R.; Lange, D.A.; Altoubat, S.A.; Rieder, K.A.; Ulreich, G.R. Fracture of plain and fiber-reinforced concrete slabs under monotonic loading. *J. Mater. Civ. Eng.* **2004**, *16*, 452–460. [CrossRef]
22. Roesler, J.R.; Altoubat, S.A.; Lange, D.A.; Rieder, K.A.; Ulreich, G.R. Effect of synthetic fibers on structural behavior of concrete slabs-on-ground. *ACI Mater. J.* **2006**, *103*, 3–10.
23. Kakooei, S.; Akil, H.M.; Jamshidi, M.; Rouhi, J. The effects of polypropylene fibers on the properties of reinforced concrete structures. *Constr. Build. Mater.* **2012**, *27*, 73–77. [CrossRef]
24. Bolat, H.; Şimşek, O.; Çullu, M.; Durmuş, G.; Can, Ö. The effects of macro synthetic fiber reinforcement use on physical and mechanical properties of concrete. *Compos. Part B Eng.* **2014**, *61*, 191–198. [CrossRef]
25. Pakravan, H.R.; Ozbakkaloglu, T. Synthetic fibers for cementitious composites: A critical and in-depth review of recent advances. *Constr. Build. Mater.* **2019**, *207*, 491–518. [CrossRef]
26. Banthia, N.; Gupta, R. Influence of polypropylene fiber geometry on plastic shrinkage cracking in concrete. *Cem. Concr. Res.* **2006**, *36*, 1263–1267. [CrossRef]
27. Alhozaimy, A.; Soroushian, P.; Mirza, F.; Alhozaimy, A.; Soroushian, P.; Mirza, F. Mechanical properties of polypropylene fiber reinforced concrete and the effects of pozzolanic materials. *Cem. Concr. Compos.* **1996**, *18*, 85–92. [CrossRef]
28. Patel, P.A.; Desai, A.K.; Desai, J.A. Evaluation of engineering properties for polypropylene fibre reinforced concrete. *Int. J. Adv. Eng. Technol.* **2012**, *3*, 42–45.
29. Yew, M.C.; Bin Mahmud, H.; Ang, B.C. Influence of different types of polypropylene fibre on the mechanical properties of high-strength oil palm shell lightweight concrete. *Constr. Build. Mater.* **2015**, *90*, 36–43. [CrossRef]
30. Nurdian, I.I.; Jalan, P.L. The prospects of using polypropylene fibers as an additive in high quality concrete. *Fiber Mesh* **1990**, 3–16.
31. Yap, S.P.; Alengaram, U.J.; Jumaat, M.Z. Enhancement of mechanical properties in polypropylene– and nylon–fibre reinforced oil palm shell concrete. *Mater. Des.* **2013**, *49*, 1034–1041. [CrossRef]
32. Labib, W.; Eden, N. *An Investigation into the Use of Fibers in Concrete Industrial Ground-Floor Slabs*; School of the Built Environment, Liverpool John Moores University: Liverpool, UK, 2006.
33. Khan, M.; Ali, K. Effectiveness of hair and wave polypropylene fibers for concrete roads. *Constr. Build. Mater.* **2018**, *166*, 581–591. [CrossRef]
34. Gali, S.; Subramaniam, K.V. Cohesive stress transfer and shear capacity enhancements in hybrid steel and macro-polypropylene fiber reinforced concrete. *Theor. Appl. Fract. Mech.* **2019**, *103*, 102250. [CrossRef]
35. Behfarnia, K.; Behravan, A. Application of high performance polypropylene fibers in concrete lining of water tunnels. *Mater. Des.* **2014**, *55*, 274–279. [CrossRef]
36. British Standards Institution (BSI). *Cement: Composition, Specifications and Conformity Criteria for Common Cements*; BS EN 197-1; BSI: London, UK, 2011.
37. Egyptian Standard Specification (ESS). *Composition, Specifications and Conformity Criteria for Common Cements*; 4576-1; Egyptian Organization for Standards and Quality (EOS): Cairo, Egypt, 2009.
38. ECP 203-2018. *Egyptian Code of Practice for Design and Construction of Reinforced Concrete Structures*; Ministry of Housing, Utilities and Urban Communities: Cairo, Egypt, 2018.
39. ASTM C494/C494M. *Standard Specification for Chemical Admixtures for Concrete*; ASTM International: West Conshohocken, PA, USA, 2019.
40. Fallah, S.; Nematzadeh, M. Mechanical properties and durability of high-strength concrete containing macro-polymeric and polypropylene fibers with nano-silica and silica fume. *Constr. Build. Mater.* **2017**, *132*, 170–187. [CrossRef]
41. ASTM C1116/C1116M-10a. *Standard Specification for Chemical Admixtures for Concrete*; ASTM International: West Conshohocken, PA, USA, 2015.
42. British Standards Institution (BSI). *Fibres for Concrete: Polymer Fibres—Definitions, Specifications and Conformity*; BS EN 14889-2; BSI: London, UK, 2006.
43. BASF-The Chemical Company. MasterFiber-249 Macrosynthetic Fiber-Product Data Sheet. 2020. Available online: https://www.master-builders-solutions.com/en-ng/products/masterfiber/masterfiber-249 (accessed on 31 August 2020).
44. Richardson, A.; Coventry, K.; Lamb, T.; MacKenzie, D. The addition of synthetic fibres to concrete to improve impact/ballistic toughness. *Constr. Build. Mater.* **2016**, *121*, 612–621. [CrossRef]
45. Alberti, M.G.; Enfedaque, A.; Gálvez, J.C.; Picazo, A. Recent advances in structural fibre-reinforced concrete focused on polyolefin-based macro-synthetic fibres. *Mater. Constr.* **2020**, *70*, 206. [CrossRef]
46. Alberti, M.G.; Enfedaque, A.; Gálvez, J.; Agrawal, V. Fibre distribution and orientation of macro-synthetic polyolefin fibre reinforced concrete elements. *Constr. Build. Mater.* **2016**, *122*, 505–517. [CrossRef]
47. Alberti, M.; Enfedaque, A.; Gálvez, J. On the mechanical properties and fracture behavior of polyolefin fiber-reinforced self-compacting concrete. *Constr. Build. Mater.* **2014**, *55*, 274–288. [CrossRef]
48. El-Newihy, A.; Azarsa, P.; Gupta, R.; Biparva, A. Effect of polypropylene fibers on self-healing and dynamic modulus of elasticity recovery of fiber reinforced concrete. *Fibers* **2018**, *6*, 9. [CrossRef]
49. Rooholamini, H.; Hassani, A.; Aliha, M. Evaluating the effect of macro-synthetic fibre on the mechanical properties of roller-compacted concrete pavement using response surface methodology. *Constr. Build. Mater.* **2018**, *159*, 517–529. [CrossRef]

50. Soutsos, M.; Le, T.; Lampropoulos, A. Flexural performance of fibre reinforced concrete made with steel and synthetic fibres. *Constr. Build. Mater.* **2012**, *36*, 704–710. [CrossRef]
51. ASTM C143/C143M. *Standard Test Method for Slump of Hydraulic-Cement Concrete*; ASTM International: West Conshohocken, PA, USA, 2020.
52. ASTM C231/C231M-17a. *Standard Test Method for Air Content of Freshly Mixed Concrete by the Pressure Method*; ASTM International: West Conshohocken, PA, USA, 2017.
53. ASTM C138/C138M-17a. *Standard Test Method for Density (Unit Weight), Yield, and Air Content (Gravimetric) of Concrete*; ASTM International: West Conshohocken, PA, USA, 2017.
54. British Standards Institution (BSI). *Testing Hardened Concrete: Compressive Strength of Test Specimens*; BS EN 12390-3; BSI: London, UK, 2009.
55. Boulekbache, B.; Hamrat, M.; Chemrouk, M.; Amziane, S. Failure mechanism of fibre reinforced concrete under splitting test using digital image correlation. *Mater. Struct.* **2014**, *48*, 2713–2726. [CrossRef]
56. ASTM C496/C496M. *Standard Test Method for Splitting Tensile Strength of Cylindrical Concrete Specimens*; ASTM International: West Conshohocken, PA, USA, 2017.
57. ASTM C293/C293M. *Standard Test Method for Flexural Strength of Concrete (Using Simple Beam with Center-Point Loading)*; ASTM International: West Conshohocken, PA, USA, 2016.
58. Hesami, S.; Hikouei, I.S.; Emadi, S.A.A. Mechanical behavior of self-compacting concrete pavements incorporating recycled tire rubber crumb and reinforced with polypropylene fiber. *J. Clean. Prod.* **2016**, *133*, 228–234. [CrossRef]
59. ASTM C469/C469M. *Standard Test Method for Static Modulus of Elasticity and Poisson's Ratio of Concrete in Compression*; ASTM International: West Conshohocken, PA, USA, 2014.
60. Hammons, M.I. *Advanced Pavement Design: Finite Element Modeling for Rigid Pavement Joints. Report II: Model Development*; MS 39180-6199; U.S. Army Engineer Waterways Experiment Station: Vicksburg, VA, USA, 1998.
61. Al-Hedad, A.S.A.; Hadi, M.N.S. Effect of geogrid reinforcement on the flexural behaviour of concrete pavements. *Road Mater. Pavement Des.* **2018**, *20*, 1005–1025. [CrossRef]
62. PCA. *US Portland Cement Association. Thickness Design for Concrete Highway and Street Pavements. Engineering Bulletin EB109P*; Portland Cement Association: Skokie, IL, USA, 1984.
63. Memon, N.A.; Sumadi, S.R.; Ramli, M. Performance of high wokability slag-cement mortar for ferrocement. *Build. Environ.* **2007**, *42*, 2710–2717. [CrossRef]
64. Chen, B.; Liu, J. Contribution of hybrid fibers on the properties of the high-strength lightweight concrete having good workability. *Cem. Concr. Res.* **2005**, *35*, 913–917. [CrossRef]
65. Wang, J.; Dai, Q.; Si, R.; Guo, S. Mechanical, durability, and microstructural properties of macro synthetic polypropylene (PP) fiber-reinforced rubber concrete. *J. Clean. Prod.* **2019**, *234*, 1351–1364. [CrossRef]
66. Alsaif, A.; Koutas, L.; Bernal, S.A.; Guadagnini, M.; Pilakoutas, K. Mechanical performance of steel fibre reinforced rubberised concrete for flexible concrete pavements. *Constr. Build. Mater.* **2018**, *172*, 533–543. [CrossRef]
67. Sahoo, D.R.; Solanki, A.; Kumar, A. Influence of steel and polypropylene fibers on flexural behavior of rc beams. *J. Mater. Civ. Eng.* **2015**, *27*, 04014232. [CrossRef]
68. Karahan, O.; Atis, C. The durability properties of polypropylene fiber reinforced fly ash concrete. *Mater. Des.* **2011**, *32*, 1044–1049. [CrossRef]
69. Olivito, R.; Zuccarello, F. An experimental study on the tensile strength of steel fiber reinforced concrete. *Compos. Part B Eng.* **2010**, *41*, 246–255. [CrossRef]
70. Hasan, M.J.; Afroz, M.; Mahmud, H.M.I. An experimental investigation on mechanical behavior of macro synthetic fiber reinforced concrete. *Int. J. Civ. Environ. Eng.* **2011**, *11*, 18–23.
71. Chorzepa, M.G.; Masud, M. Performance of multiscale, including nanoscale, fibres in concrete. *Emerg. Mater. Res.* **2017**, *6*, 198–209. [CrossRef]
72. Saadun, A.; Mutalib, A.A.; Hamid, R.; Mussa, M.H. Behaviour of polypropylene fiber reinforced concrete under dynamic impact load. *J. Eng. Sci. Technol.* **2016**, *11*, 684–693.
73. Hsie, M.; Tu, C.; Song, P. Mechanical properties of polypropylene hybrid fiber-reinforced concrete. *Mater. Sci. Eng. A* **2008**, *494*, 153–157. [CrossRef]
74. Berndt, M.L. Properties of sustainable concrete containing fly ash, slag and recycled concrete aggregate. *Constr. Build. Mater.* **2009**, *23*, 2606–2613. [CrossRef]
75. Foti, D. Preliminary analysis of concrete reinforced with waste bottles PET fibers. *Constr. Build. Mater.* **2011**, *25*, 1906–1915. [CrossRef]
76. Gao, J.; Sun, W.; Morino, K. Mechanical properties of steel fiber-reinforced, high-strength, lightweight concrete. *Cem. Concr. Compos.* **1997**, *19*, 307–313. [CrossRef]
77. Wu, F.; Liu, C.; Diao, Z.; Feng, B.; Sun, W.; Li, X.; Zhao, S. Improvement of mechanical properties in polypropylene- and glass-fibre-reinforced peach shell lightweight concrete. *Adv. Mater. Sci. Eng.* **2018**, *2018*, 6250941. [CrossRef]
78. Sabih, G.; Tarefder, R.A. Impact of variability of mechanical and thermal properties of concrete on predicted performance of jointed plain concrete pavements. *Int. J. Pavement Res. Technol.* **2016**, *9*, 436–444. [CrossRef]
79. Kamel, M.A. Quantification of benefits of steel fiber reinforcement for rigid pavement. *Am. J. Civ. Eng. Archit.* **2016**, *4*, 189–198.